The Hydrothermal Synthesis, Crystal Structures and Thermal Stability of the Novel One- and Two-Dimensional Thioantimonate(III) Compounds $[Co(tren)]Sb_2S_4$ and $[Ni(tren)]Sb_2S_4$

Ralph Stähler[a] and Wolfgang Bensch*[a]

Keywords: Sulfur / Antimony / Solvothermal synthesis / Crystal structure / Thermoanalytical measurements

Two novel thioantimonate(III) compounds $[Co(C_6H_{18}N_4)]Sb_2S_4$ (**1**) and $[Ni(C_6H_{18}N_4)]Sb_2S_4$ (**2**) were synthesised under solvothermal conditions by reacting the transition metal, Sb and S in a 50% solution of tris(2-aminoethyl)amine (tren). The use of a tetradentate amine yields incompletely shielded transition metal cations which in turn are able to form bonds to the sulfur atoms of thioantimonate(III) anions. Compound **1** crystallises in the orthorhombic space group *Pbca*, a = 13.886(3) Å, b = 11.452(2) Å, c = 20.549(4) Å, V = 3268(1) Å^3, Z = 8 and compound **2** crystallises in the monoclinic space group $P2_1/n$, a = 6.906(1) Å, b = 22.822(5) Å, c = 10.347(2) Å, β = 103.17(3)°, V = 1587.9(6) Å^3, Z = 4. The $^2_\infty[Sb_2S_4^{2-}]$ anion in compound **1** is formed by an SbS_3 and an SbS_4 unit sharing a common corner. Two SbS_4 units have a common edge to form an Sb_2S_2 heterocycle. Four such Sb_2S_2 rings are at the corners of a two-dimensional square-like net. Interconnection of the rings by SbS_3 pyramids yields $Sb_{10}S_{10}$ rings with pores measuring 10·8.4 Å in diameter. The pores are filled by the $[Co(tren)]^{2+}$ cations. The $[Co]^{2+}$ cation is in a trigonal bipyramidal environment of four N atoms of the tren ligand and one S atom of the SbS_3 pyramid. The one-dimensional $^1_\infty[Sb_2S_4^{2-}]$ chain anion in **2** is built by two corner-sharing SbS_3 units. The $[Ni]^{2+}$ cation is in an octahedral environment consisting of four N atoms of the tren ligand and two S atoms of the anion. An $NiSb_2S_3$ heteroring in a twist conformation is formed with an unusually large Ni–S(1)–Sb(1) angle of 121.73(3)°. For the $[Co]^{2+}$ (d^7) cation no significant energy differences can be expected for the trigonal bipyramidal and octahedral coordination, and due to the geometrical requirements of the tetradentate ligand the former environment is preferred. In contrast, for $[Ni]^{2+}$ (d^8) an octahedral environment is energetically favoured over the trigonal bipyramidal arrangement. Both compounds start to decompose under an Ar atmosphere at about 250 °C. For **1** two not well resolved steps are observed, whereas **2** decomposes in one step. In the X-ray powder patterns of the grey products Sb_2S_3, Co/NiSbS and Co/NiS could be identified.

Introduction

Compared to the large number of thioantimonate(III) compounds with A^+ (A = alkali metal), EA^{2+} (EA = earth alkali metal) or organic ammonium cations as charge balancing ions only a few compounds are known in which a transition metal is integrated within the anionic framework of the main group thiometallates. In $[M(NH_3)_6]Cu_8Sb_3S_{13}$ the Cu_8S_{13} cores are linked by Sb atoms resulting in the formation of channels that are occupied by transition metal hexamine complexes.[1] Adamantane-like $[Ge_4S_{10}]^{4-}$ units have been linked by tetrahedral Mn^{II},[2] copper[3] or dimers like $[Ag_2]^+$ and $[Cu_2]^+$.[4] Other examples are copper antimony sulfides prepared at elevated temperatures such as $Cu_{12}Sb_4S_{13}$,[5] Cu_3SbS_4,[6] Cu_3SbS_3,[7–9] $CuSbS_2$,[10] and $[Cu_2SbS_3]\cdot(en)_{0.5}$ synthesised by the solvothermal route.[11] Applying solvothermal conditions it was also possible to incorporate a complex cation $[Co(en)_3]^{2+}$ into a thioantimonate(III) framework.[12] During the last few years we have synthesised and characterised layered thioantimonates(III) with general formula $Mn_2Sb_2S_5\cdot L$ (L = methylamine, ethylamine, 1,3-diaminopropane, *N*-methyl-1,3-diaminopropane and diethylenetriamine) with Mn^{II} being part of the Sb_2S_5 network.[13–15]

For syntheses using elements as starting materials very basic solutions are needed to dissolve and mobilise the elements. Organic amines are useful solvents with high pH values. However, the amines usually coordinate to the transition metal cations (TM^{n+}) preventing their incorporation into the thioantimonate(III) network. A way of enhancing the probability that the TM^{n+} ions are integrated into the thiometallate network is the use of multidentate amines which coordinate the TM^{n+} ion but leave one or two coordination sites free for bonds to the S atoms of the M_xS_y moieties (M = main group element). According to this idea the tetradentate amine tris(2-aminoethyl)amine (tren) seems to be a good candidate: transition metal cations that prefer an octahedral environment are coordinated by the four N atoms of the tren ligand leaving two coordination sites to form bonds to the S atoms of the thiometallate framework. Such ligated $[TM(tren)]^{n+}$ complexes may be described as geometrically constrained structure-directing agents.

Based on these considerations we synthesised and characterised two novel thioantimonate(III) compounds, two-dimensional $[Co(tren)]Sb_2S_4$ and one-dimensional $[Ni(tren)]Sb_2S_4$, both exhibiting new and exciting thioantimonate(III) networks.

[a] Institut für Anorganische Chemie, Universität Kiel
Olshausenstraße 40, 24098 Kiel, Germany
Fax: (internat.) + 49-(0)431/880-1520
E-Mail: wbensch@ac.uni-kiel.de

  1434–1948/01/1212–3073 $ 17.50+.50/0

Results and Discussion

In the new compound $[Co(tren)]Sb_2S_4$ (**1**) the $[Co]^{2+}$ ion is coordinated by four N atoms of the tren ligand, with Co−N distances ranging from 2.077(2) to 2.263(2) Å (see Table 1) and by one S atom of the $^2_\infty[Sb_2S_4^{2-}]$ anion yielding a trigonal bipyramidal environment (Figure 1). As expected the longer Co−N(1) bond is *trans* to the Co−S(1) bond [distance: 2.3539(7) Å].[14] The $^2_\infty[Sb_2S_4^{2-}]$ anion is built up from the Sb(1) and Sb(2) atoms, each being in a different geometrical environment of S atoms. The Sb(1) atom has bonds to three S atoms [S(1) to S(3)] forming the typical SbS_3 trigonal pyramid. The Sb(1)−S bond lengths are between 2.3899(7) and 2.4655(6) Å, indicating single bonds. The S(1) atom of the $Sb(1)S_3$ pyramid has a bond to the $[Co]^{2+}$ ion and the two other S atoms are bound to the Sb(2) atom. The Sb(2) atom has a shorter bond to S(3) [2.4577(7) Å] and a longer bond of 2.8784(8) Å to S(2a). The environment of Sb(2) is completed by S(4) at a distance of 2.3991(8) Å and the symmetry related S(4b) atom at 2.7084(7) Å yielding an $Sb(2)S_4$ unit. The two long Sb(2)−S distances are longer than expected for single bonds, which usually lie between about 2.4 and 2.6 Å, but they are significantly shorter than the typical so-called secondary bonds with Sb−S distances above about 2.9 Å. The two long Sb(2)−S bonds are in *trans* position to each other [angle: S(2a)−Sb(2)−S(4b): 174.95(2)°]. Taking into account the Sb^{III} $6s^2$ lone pair the environment may be described as distorted trigonal bipyramidal. We note that SbS_4 units are not uncommon and Sb−S distances between 2.4 and 2.85 Å were reported, for example, for $Cs_2Sb_8S_{13}$,[17] $(CH_3NH_3)_2Sb_8S_{13}$,[18] $Cs_5Sb_8S_{18}(HCO_3)$,[19] and $[Fe(C_4H_{13}N_3)_2]Sb_6S_{10}\cdot 0.5H_2O$.[20]

Two $Sb(2)S_4$ units share a common edge to form an Sb_2S_2 heteroring. Four such Sb_2S_2 heterorings are at the corners of a square-like net and are each joined by four $Sb(1)S_3$ pyramids yielding a two-dimensional thioantimonate(III) layer within the *ab* plane (Figure 2). The interconnection of the Sb_2S_2 rings and the pyramids yields large $Sb_{10}S_{10}$ rings with pores having a diameter of 10.19 × 8.388 Å (shaded area in Figure 2) measured between symmetry related Sb(1) atoms. The cavities of the rings are filled by the $[Co(tren)]^{2+}$ cations.

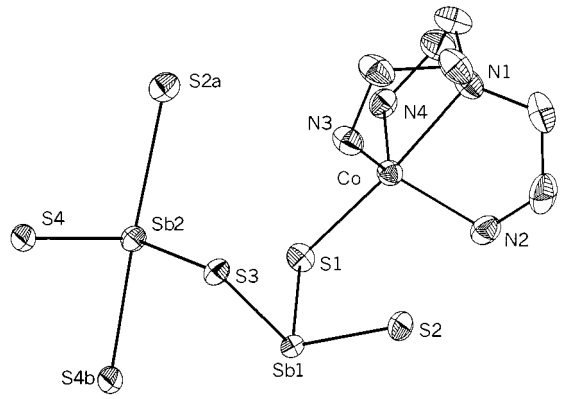

Figure 1. View of the $[Co(tren)]Sb_2S_4$ unit with labelling and displacement ellipsoids drawn at the 50% probability level; the symmetry codes are given in Table 1; hydrogen atoms are omitted for clarity

Table 1. Selected distances [Å] and angles [°] for $[Co(tren)]Sb_2S_4$

Sb(1)−S(1)	2.4165(7)	Sb(1)−S(2)	2.3899(7)
Sb(1)−S(3)	2.4655(6)	Sb(2)−S(2)[a]	2.8784(8)
Sb(2)−S(3)	2.4577(7)	Sb(2)−S(4)	2.3991(8)
Sb(2)−S(4)[b]	2.7084(7)	Co−S(1)	2.3539(7)
Co−N(1)	2.263(2)	Co−N(2)	2.077(2)
Co−N(3)	2.082(2)	Co−N(4)	2.092(2)
S(1)−Sb(1)−S(2)	103.05(2)	S(1)−Sb(1)−S(3)	96.53(2)
S(2)−Sb(1)−S(3)	95.71(3)	S(2)[a]−Sb(2)−S(3)	88.31(2)
S(2)[a]−Sb(2)−S(4)	93.39(2)	S(2)[a]−Sb(2)−S(4)[b]	174.95(2)
S(3)−Sb(2)−S(4)	99.15(2)	S(3)−Sb(2)−S(4)[b]	93.38(3)
S(4)−Sb(2)−S(4)[b]	91.04(2)	Co−S(1)−Sb(1)	106.95(3)
N(1)−Co−S(1)	175.32(6)	N(2)−Co−S(1)	105.35(7)
N(3)−Co−S(1)	98.38(6)	N(4)−Co−S(1)	98.70(6)
N(1)−Co−N(2)	79.30(9)	N(1)−Co−N(3)	79.37(8)
N(1)−Co−N(4)	79.11(8)	N(2)−Co−N(3)	120.85(9)
N(2)−Co−N(4)	108.54(8)	N(3)−Co−N(4)	120.36(9)
long Sb−S bonds [Å]			
Sb(1)−S(4)[b]	3.6103(8)	Sb(2)−S1	3.4765(9)

[a] Symmetry code: $0.5 - x$, $0.5 + y$, z. − [b] $-x$, $1 - y$, $-z$.

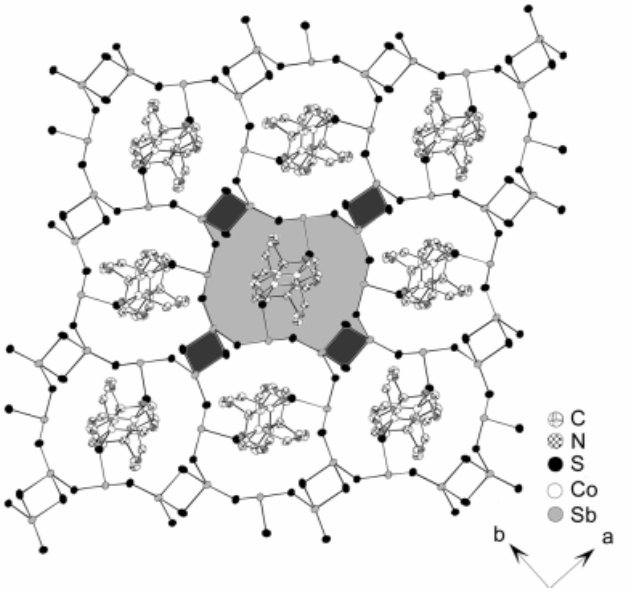

Figure 2. The crystal structure of $[Co(tren)]Sb_2S_4$ viewed along [001]; the Sb_2S_2 and the $Sb_{10}S_{10}$ heterorings are highlighted by shaded areas; the probability ellipsoids are drawn at the 50% level; hydrogen atoms are omitted for clarity

The layers are stacked parallel to the *c* axis to form channels containing the cations, with H···S contacts between 2.566 and 2.723 Å and angles N−H···S ranging from 150.24 to 164.63° indicating weak hydrogen bonding (Table 2).

Table 2. Selected H···S distances [Å] and angles [°]

$[Co(tren)]Sb_2S_4$				$[Ni(tren)]Sb_2S_4$			
N2−H1N2	2.566	154.30	S1[a]	N1−H2N1	2.594	146.62	S1[b]
N3−H2N3	2.723	164.63	S2[c]	N4−H1N4	2.834	161.26	S1[b]
N4−H1N4	2.626	150.24	S3[c]	N1−H1N1	2.615	166.86	S4[d]

[a] Symmetry code: $-x+1, -y+1, -z$. − [b] $-x+1, -y, -z+1$. − [c] $-x+1/2, y+1/2, z$. − [d] $x+1, y, z$.

The Sb atoms complete their coordination spheres by so-called secondary bonds to S atoms: one contact is observed for Sb(1) [3.6103(8) Å to S(4b)] and one for Sb(2) [3.4765(9) Å to S(1)] (Figure 3: A and B; Table 1). Taking these contacts into account the environment of Sb(1) may be viewed as a ψ-trigonal bipyramid (Figure 3, A) and that of Sb(2) as a distorted ψ-octahedron (Figure 3, B).

In $[Ni(tren)]Sb_2S_4$ the $[Ni]^{2+}$ ion is coordinated by four N atoms of the tren ligand with Ni−N distances ranging between 2.085(2) and 2.115(2) Å (see Table 3) and by two S atoms of the $^1_\infty[Sb_2S_4^{2-}]$ anion, yielding an octahedral coordination (Figure 4). The Ni−N bond lengths lie within the range reported in the literature.[21−23] The Ni−S bond lengths are 2.4306(8) Å for Ni−S(1) and 2.642(1) Å for Ni−S(4). An analysis of the geometry about the cation reveals why the Ni−S(4) distance is elongated: the S(1) and S(4) atoms have neighbouring N atoms at a distance of about 3.2−3.5 Å. A shortening of the Ni−S(4) bond to about 2.4 Å would bring the S(4) atom in closer contact to the N atoms leading to strong repulsive interactions. To avoid these repulsive forces the geometry at the $[Ni]^{2+}$ centre, as well as that of the anion, must be distorted, which is energetically unfavourable.

The thioantimonate(III) anion acts as a bidentate ligand to form an $NiSb_2S_3$ heteroring exhibiting the twist conformation (Figure 4). An interesting feature within the ring is the relatively large Ni−S(1)−Sb(1) angle of 121.73(3)°. In the overwhelming number of cases the angles around the

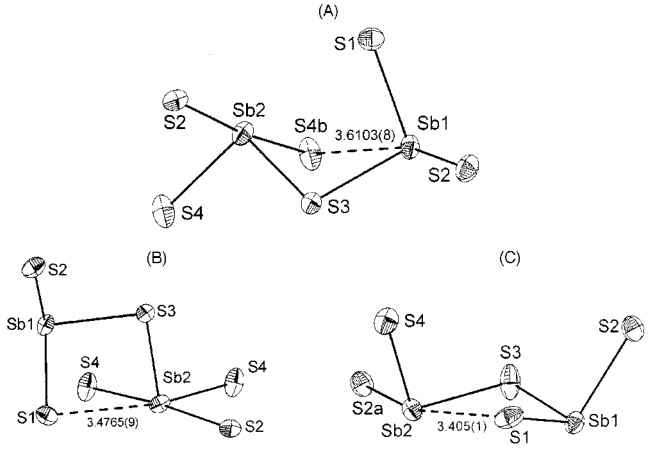

Figure 3. The environments of the Sb atoms with their long secondary bonds (dotted lines); (A and B) $[Co(tren)]Sb_2S_4$; (C) $[Ni(tren)]Sb_2S_4$; the numbers are the interatomic distances in Å

Table 3. Selected distances [Å] and angles [°] for $[Ni(tren)]Sb_2S_4$

Sb(1)−S(1)	2.3676(9)	Sb(1)−S(2)	2.4652(8)
Sb(1)−S(3)	2.4456(9)	Sb(2)−S(2)[a]	2.486(1)
Sb(2)−S(3)	2.4599(9)	Sb(2)−S(4)	2.3549(8)
Ni−S(1)	2.4306(8)	Ni−S(4)	2.642(1)
Ni−N(1)	2.097(2)	Ni−N(2)	2.115(2)
Ni−N(3)	2.085(2)	Ni−N(4)	2.105(2)
S(1)−Sb(1)−S(2)	103.03(3)	S(1)−Sb(1)−S(3)	100.19(4)
S(2)−Sb(1)−S(3)	93.16(3)	S(2)[a]−Sb(2)−S(3)	89.89(3)
S(2)[a]−Sb(2)−S(4)	97.02(3)	S(3)−Sb(2)−S(4)	102.03(3)
Ni−S(1)−Sb(1)	121.73(3)	Sb(1)−S(2)−Sb(2)[b]	96.27 (3)
Sb(1)−S(3)−Sb(2)	98.34(3)	Sb(2)−S(4)−Ni	102.64(3)
N(1)−Ni−N(2)	82.03(9)	N(1)−Ni−N(3)	94.1(1)
N(1)−Ni−N(4)	92.3(1)	N(2)−Ni−N(3)	83.6(1)
N(2)−Ni−N(4)	82.5(1)	N(3)−Ni−N(4)	163.8(1)
N(1)−Ni−S(1)	90.39(7)	N(2)−Ni−S(1)	169.95(7)
N(3)−Ni−S(1)	103.62(7)	N(4)−Ni−S(1)	91.22(8)
N(1)−Ni−S(4)	173.81(7)	N(2)−Ni−S(4)	91.79(7)
N(3)−Ni−S(4)	84.74(8)	N(4)−Ni−S(4)	87.23(8)
S(1)−Ni−S(4)	95.79(3)		
long Sb−S bonds [Å]			
Sb(2)−S(1)	3.405(1)		

[a] Symmetry code: $-1+x, y, z$. − [b] $1+x, y, z$.

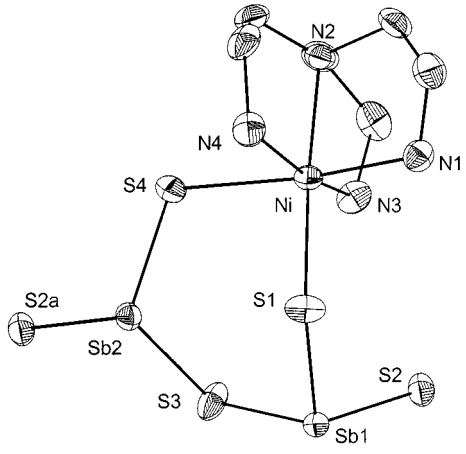

Figure 4. $[Ni(tren)]Sb_2S_4$ with the $NiSb_2S_3$ heteroring, labelling and displacement ellipsoids drawn at the 50% level; the hydrogen atoms are omitted for clarity

S atoms are between about 90 and 110°. For silicates, strong deviations of the Si−O−Si angles from the strain-free angle of about 140° are accompanied by an enhanced isotropic (U_{eq}) and/or anisotropic displacement parameter.[24] For S(1) the U_{eq} is comparable with those of the other atoms, but the U_{11} parameter is more than twice the U_{22} and U_{33} components. However, it should be noted that the U_{22} of S(3) is also large despite a relatively "normal" Sb(1)−S(3)−Sb(2) angle of 98.34(3)°, hence a straightforward relationship as for silicates is not obvious, and a rigorous analysis of many such thioantimonates(III) is required to establish such a relationship.

The anionic part of the structure, $^1_\infty[Sb_2S_4^{2-}]$, is composed of two corner-sharing SbS_3 pyramids formally yielding an Sb_2S_5 unit. The Sb−S distances are between

2.3549(8) and 2.486(1) Å, typical for single bonds. The Sb_2S_5 unit is interconnected via the S(2) atom into one-dimensional chains running parallel to the *a* axis (see Figure 5). These chains are arranged in a simple hexagonal rod packing. The coordination sphere of Sb(2) is completed by a secondary bond to S(1) of 3.405(1) Å forming a distorted ψ-trigonal bipyramid (Figure 3, C; Table 3). For the Sb(1) atom no S atoms are found at distances less than 4 Å. Three short intermolecular H···S distances (Table 2) with distances ranging from 2.594 to 2.834 Å and N−H···S angles between 146.62° and 166.86° are observed, which may indicate weak hydrogen bonding.

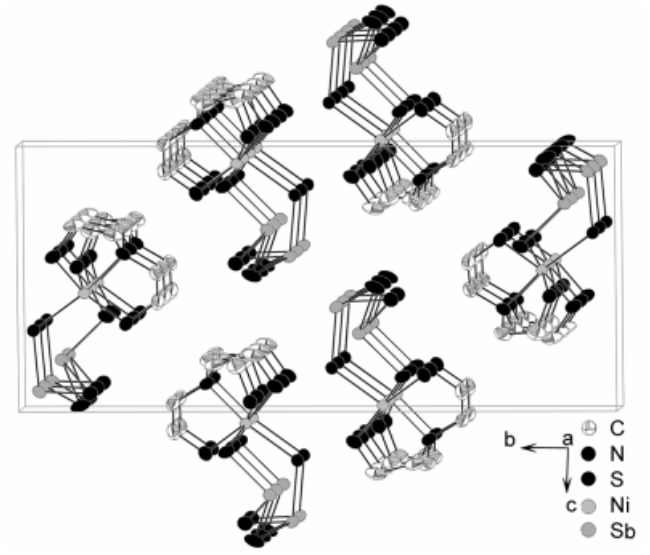

Figure 5. Crystal structure of [Ni(tren)]Sb_2S_4 viewed along [100]; the probability ellipsoids are drawn at the 50% level; hydrogen atoms are omitted for clarity

The $[Co]^{2+}$ cation has a d^7 electronic configuration. Simple considerations suggest that the energy differences between the trigonal bipyramidal and octahedral coordination should be negligible. Therefore, it can be assumed that the geometrical requirements of the tetradentate ligand force the formation of the trigonal bipyramidal environment. For $[Ni]^{2+}$, with a d^8 electronic configuration, the octahedral environment is energetically favoured over the trigonal bipyramidal arrangement.

Thermal Investigations

[Co(tren)]Sb_2S_4: The DTA-TG curve is shown in Figure 6. Decomposition starts at T_{onset} = 262 °C. A weight loss occurs in two steps on heating. These steps are accompanied by two strong endothermic signals in the DTA curve with peak temperatures T_p = 270 °C and T_p = 295 °C. The total loss of weight amounts to $-\Delta m_{1+2}$ = 23.8% ($-\Delta m_1$ = 15.8%, $-\Delta m_2$ = 8%). If the tren ligand is extruded during thermal decomposition a value of $-\Delta m_{theo(tren)}$ = 25.3% is expected. C, H and N were all found in the grey residue (C: 0.4%; H: 0.5%; N: 0.2%; CHN_{sum} = 1.1%) suggesting that the decomposition reaction is more complex. In the decomposition product Sb_2S_3, CoS and CoSbS was identified by X-ray powder diffraction (XRD).

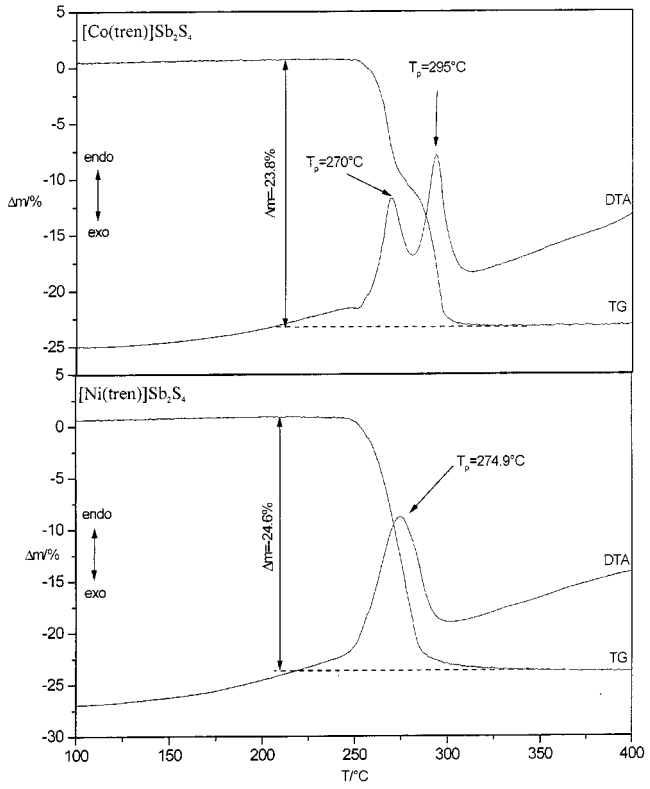

Figure 6. DTA and TG curves of [Co(tren)]Sb_2S_4 (atmosphere: argon; weight: 75.10 mg powdered crystals; heating rate: 3 °C/min) and [Ni(tren)]Sb_2S_4 (atmosphere: argon; weight: 68.50 mg; heating rate: 3 °C/min; T_p = peak temperature)

In a further experiment the decomposition was stopped at 270 °C. In the X-ray powder pattern Sb_2S_3, CoS, CoSbS and a small amount of a fourth phase were identified. The weight loss between T_p = 270 °C and T_p = 295 °C may be attributed to the decomposition of the unknown phase accompanied by the emission of C, H and N as well as S (C: 5.061%; H: 0.876%; N: 3.242%; CHN_{sum} = 9.179%). In the IR spectrum of the residue no C−H, C−N, C−C or N−H vibrations could be detected.

[Ni(tren)]Sb_2S_4: A significantly different behaviour is observed for the Ni compound. As can be seen in Figure 6 the sample decomposes in one step with an endothermic signal in the DTA curve at T_p = 274.9 °C (T_{onset} = 254 °C). The loss of weight is $-\Delta m$ = 24.6% which is similar to the value calculated for the emission of the tren ligand ($-\Delta m_{theo(tren)}$ = 25.4%). In the black residue small amounts of C, H and N could be found (C: 0.3%; H: 0.3%; N: 0.2%; CHN_{sum} = 0.8%). No C−H, C−N, C−C or N−H vibrations could be detected in the IR spectrum. NiS, Sb_2S_3 and NiSbS could be identified by X-ray powder diffraction.

Raman Spectroscopy

The changes of the bonding properties of a lone pair atom are best detected from changes in the bond angles, as interatomic bond lengths are only affected slightly.[25,26]

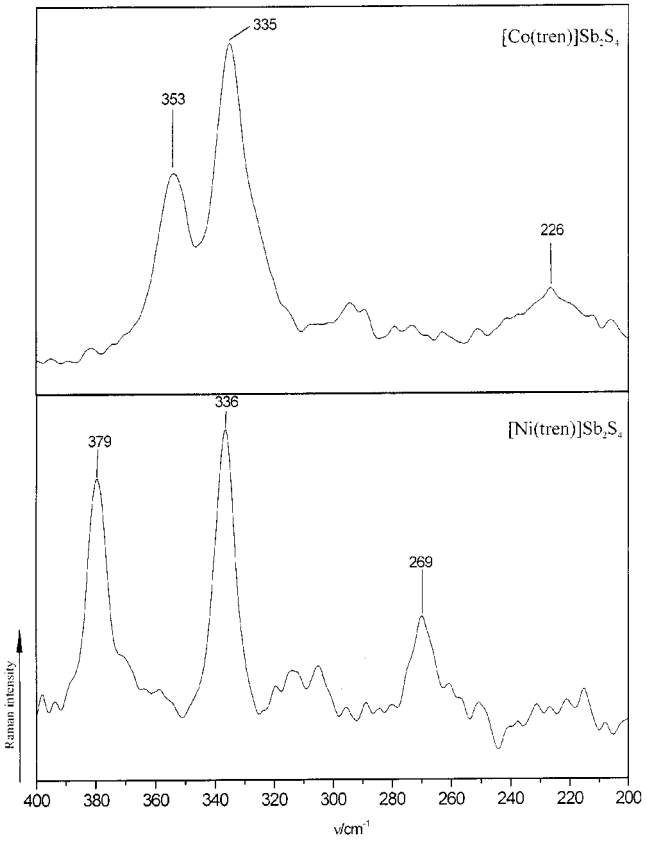

Figure 7. Raman spectra of $[Co(tren)]Sb_2S_4$ and $[Ni(tren)]Sb_2S_4$

This means that the local environment of the Sb^{III} ions does not lead to significant alterations of the Sb−S distances. In the Raman spectra, however, the different bonding properties of the two title compounds become apparent (Figure 7). For $[Co(tren)]Sb_2S_4$ two intense bands located at 353 and 335 cm^{-1} are observed, in accordance with the observation that all Sb^{III} ions have a $(3 + n)$ coordination [$n = 1$ for Sb(1) and $n = 2$ for Sb(2)]. For the Ni compound one Raman band is located at 379 cm^{-1} which can be assigned to $Sb(1)S_3$; a band at lower frequency of 336 cm^{-1} is due to the $Sb(2)S_4$ unit. The lower Raman frequencies obtained for the Co compound reflect the decreased bonding interactions within the $[SbS_3^{3-}]$ units. The Raman bands at 226 cm^{-1} (Co compound) and 269 cm^{-1} (Ni compound) are assigned to Co−S/Ni−S vibrations. The assignment of the Sb−S modes is in accordance with the results reported by Pfitzner for Cu_3SbS_3 and $(CuI)_2Cu_3SbS_3$.[27] In the former compound two maxima were observed at 321 and 290 cm^{-1} reflecting the weaker bonding interaction due to the (3 + 5) environment. In the latter compound the $[SbS_3^{3-}]$ anion has no next-nearest S atoms, yielding Raman bands at 362 and 339 cm^{-1}. For $Mn_2Sb_2S_4$ with one Sb^{III} atom in a sixfold and the other Sb^{III} atom in a sevenfold environment of S atoms the Raman bands occur at even lower frequencies and are located between about 280 and 310 cm^{-1}.[28]

Experimental Section

Synthesis: $[Ni(tren)]Sb_2S_4$ was first prepared by reacting elemental Ni, Sb and S in an aqueous solution of tren under solvothermal conditions in a Teflon-lined steel autoclave (inner volume: 30 mL). In a typical synthesis 1 mmol of Ni (0.0586 g), 1 mmol of Sb (0.1217 g) and 3 mmol of S (0.0962 g) were added to 10 mL of a 50% aqueous tren solution. The mixture was heated at 140 °C for 8 days then cooled to room temperature within 3 h. The reaction mixture was filtered, washed with water and acetone and cleaned in an ultrasonic bath. The product consists of green square-like crystals of the title compound as the major phase and a grey microcrystalline powder as the minor phase which is amorphous to X-rays. In the by-product the elements Ni, S, and Sb were identified by an EDAX analysis. Stirring the reaction mixture during the synthesis gave a phase-pure product using the same ratio of starting materials as under static conditions. C, H N analysis: calcd. C 12.49, H 3.15, N 9.72; found C 12.24, H 3.05, N 9.60.

$[Co(tren)]Sb_2S_4$: Dark black squares of $[Co(tren)]Sb_2S_4$ were prepared by reacting a mixture of elemental Co (0.059 g, 1 mmol), Sb (0.121 g, 1 mmol) and S (0.096 g, 3 mmol) in an aqueous solution of 50% tren (10 mL) (Merck Chemical). The synthesis was performed in a Teflon-lined steel autoclave, which was heated to 140 °C, held at this temperature for 7 days and then cooled to room temperature within 3 h. The products were filtered off, washed with water and dried under vacuum. The yield was 70% based on Co. Stirring the solution during the synthesis gave nearly 100% yield based on Co (Co/Sb/S = 1:1:3) in an aqueous solution of 10 mL tren (50%) at 140 °C. Calcd. C 12.49, H 3.14, N 9.71; found C 12.14, H 3.14, N 9.17. NB The differences between the applied starting material ratio and the 1:2:4 ratio in the solid products is due to unknown antimony sulfide species dissolved in the solution.

Structure Determination: Intensities were collected on a STOE Imaging Plate Diffraction System (IPDS) and a STOE AED-II four-circle diffractometer using monochromated Mo-K_α radiation (λ = 0.71073 Å). The intensities were corrected for Lorentz, polarisation and absorption effects. Structure solution was performed using SHELXS-97.[29] Refinement was done against F^2 using SHELXL-97.[30] All heavy atoms were refined anisotropically. The hydrogen atoms were positioned with idealised geometry and refined with fixed isotropic displacement parameters using a riding model. Technical details of data acquisition and refinement results are summarised in Table 4.

Thermoanalytical Measurements: Thermoanalytical measurements were performed using a DTA-TG device STA 429 from Netzsch. All measurements were performed under an argon atmosphere (flow rate 50 mL min^{-1}) with Al_2O_3 crucibles and heating rates of 3 K min^{-1}.

Raman Spectroscopy: Raman spectra were measured in the region from 100 to 3500 cm^{-1} with a Bruker IFS 66 Fourier transform Raman spectrometer (wavelength: 514.5 nm, 20 K).

X-ray Powder Diffractometry: The X-ray powder patterns were recorded on a STOE Stadi-P diffractometer (Co-$K_{\alpha 1}$, Cu-$K_{\alpha 1}$ radiation, λ = 1.788965 and 1.540598 Å, respectively) in transmission geometry.

Crystallographic data (excluding structure factors) for the structures reported in this paper have been deposited with the Cambridge Crystallographic Data Centre as supplementary publication nos. CCDC-162040 for $[Ni(tren)]Sb_2S_4$ and CCDC-162041 for $[Co(tren)]Sb_2S_4$. Copies of the data can be obtained free of charge on application to CCDC, 12 Union Road, Cambridge

Table 4. Technical details of data acquisition and selected refinement results for $[Co(tren)]Sb_2S_4$ and $[Ni(tren)]Sb_2S_4$

Empirical formula	$[Co(C_6H_{18}N_4)]Sb_2S_4$	$[Ni(C_6H_{18}N_4)]Sb_2S_4$
Colour, habit	black squares	dark green squares
Crystal size	0.3 × 0.1 × 0.1 mm	0.3 × 0.02 × 0.1 mm
Molecular weight	576.91 g/mol	576.69 g/mol
Crystal system	orthorhombic	monoclinic
Space group	*Pbca*	$P2_1/n$
Calculated density	2.345 g/cm^3	2.412 g/cm^3
a	13.886(3) Å	6.906(1) Å
b	11.452(2) Å	22.822(5) Å
c	20.549(4) Å	10.347(2) Å
β	90.00 °	103.17(3) °
V	3267.9(11) A^3	1587.9(6) A^3
Z	8	4
Temperature	293 *K*	293 *K*
Scan range	$5° \leq 2\theta \leq 56°$	$5.4° \leq 2\theta \leq 56°$
	$-17 \leq h \leq 18$	$0 \leq h \leq 9$
	$-15 \leq k \leq 15$	$0 \leq k \leq 30$
	$-24 \leq l \leq 25$	$-13 \leq l \leq 13$
Measured reflections	31348	4246
Independent reflections	3766	3827
Reflections with $F_o > 4\sigma(F_o)$	3345	3251
μ	4.78 mm^{-1}	5.06 mm^{-1}
$R_{int.}$	0.030	0.016
Absorption correction	face-indexed	face-indexed
Min./max. trans.	0.3609/0.5848	0.3693/0.6770
Extinction coefficient[a]	none	$x = 0.00050(10)$
Weight[b]	$y = 0.0242$, $z = 2.1033$	$y = 0.0205$, $z = 0.7594$
*R*1 $[F_o > 4\sigma(F_o)]$	0.0197	0.0187
*R*1 (all reflections)	0.0249	0.0306
*wR*2 $[F_o > 4\sigma(F_o)]$	0.0437	0.0449
*wR*2 (all reflections)	0.0456	0.0468
Δρ	−0.67/0.66 e/Å^3	−0.41/0.71 e/Å^3
Goodness of fit	1.072	1.038

[a] $F^* = F_c(k[1 + 0.001 \cdot x \cdot F_c^2 \cdot \lambda^3/\sin(2\theta)]^{-0.25})$. − [b] $w = 1/[\sigma^2(F_o^2) + (yP)^2 + zP]$; $P = (\max(F_o^2,0) + 2F_c^2)/3$.

CB2 1EZ, UK [Fax: (internat.) +44-1223/336-033; E-mail: deposit@ccdc.cam.ac.uk].

Acknowledgments

This work has been supported by the State of Schleswig-Holstein and the Fonds der Chemischen Industrie.

[1] G. L. Schimek, J. W. Kolis, G. J. Long, *Chem. Mater.* **1997**, *9*, 2776−2785.
[2] C. L. Cahill, J. B. Parise, *Chem. Mater.* **1997**, *9*, 807−811.
[3] K. Tan, A. Darovsky, J. B. Parise, *J. Am. Chem. Soc.* **1995**, *117*, 7039−7040.
[4] C. L. Bowes, W. U. Huynh, S. J. Kirkby, A. Malek, G. A. Ozin, S. Petrov, M. Twardowski, D. Young, R. L. Bedard, T. Broach, *Chem. Mater.* **1996**, *8*, 2147−2152.
[5] A. Pfitzner, M. Evain, V. Petricek, *Acta Crystallogr., Sect. B* **1997**, *53*, 337−345.
[6] J. Garin, E. Parthe, H. R. Oswald, *Acta Crystallogr., Sect. B* **1972**, *28*, 3672−3674.
[7] A. Pfitzner, *Z. Anorg. Allg. Chem.* **1994**, *620*, 1992−1997.
[8] S. Karup-Møller, E. Makovicky, *Am. Mineral.* **1974**, *59*, 889−895.
[9] E. Makovicky, T. Balic-Zunic, *Can. Mineral.* **1995**, *33*, 655−663.
[10] M. F. Razmara, C. M. B. Henderson, R. A. D. Pattrick, *Mineral. Mag.* **1997**, *61*, 79−88.
[11] A. V. Powell, S. Boissiere, A. M. Chippindale, *J. Chem. Soc., Dalton Trans.* **2000**, *22*, 4192−4195.
[12] H.-O. Stephan, M. G. Kanatzidis, *J. Am. Chem. Soc.* **1996**, *118*, 12226−12227.
[13] W. Bensch, M. Schur, *Eur. J. Solid State Inorg. Chem.* **1996**, *33*, 1149−1160.
[14] M. Schur, C. Näther, W. Bensch, *Z. Naturforsch.* **2001**, *56b*, 79−84.
[15] L. Engelke, R. Stähler, M. Schur, C. Näther, W. Bensch, *Z. Anorg. Allg. Chem.* **2001**, in preparation.
[16] R. Demuth, F. Kober, Grundlagen der Komplexchemie, Frankfurt am Main, **1992**, *2*, 145−150.
[17] K. Volk, H. Schäfer, *Z. Naturforsch.* **1979**, *34b*, 1637−1640.
[18] X. Wang, F. Liebau, *J. Solid State Chem.* **1994**, *111*, 385−389.
[19] G. L. Schimek, J. W. Kolis, *Inorg. Chem.* **1997**, *36*, 1689−1693.
[20] R. Stähler, C. Näther, W. Bensch, *Eur. J. Inorg. Chem.* **2001**, *7*, 1835−1840.
[21] W. Bensch, C. Näther, R. Stähler, *Chem. Commun.* **2001**, *5*, 477−478.
[22] J. Ellermeier, W. Bensch, *Monatsh. Chem.* **2001**, *132*, 565−573.
[23] R. Stähler, C. Näther, W. Bensch, *Acta Crystallogr., Sect. C* **2001**, *57*, 26−27.
[24] F. Liebau, Structural Chemistry of Silicates, Springer Verlag, Germany, **1985**, p. 24 ff.
[25] X. Wang, F. Liebau, *Acta Crystallogr., Sect. B* **1996**, *52*, 7−15.
[26] X. Wang, F. Liebau, *Z. Kristallogr.* **1996**, *211*, 437−439.
[27] A. Pfitzner, *Chem. Eur. J.* **1997**, *3*, 2032−2038.
[28] A. Pfitzner, D. Kurowski, *Z. Kristallogr.* **2000**, *215*, 373−376.
[29] G. M. Sheldrick, *SHELXS-97*, Universität Göttingen, **1997**.
[30] G. M. Sheldrick, *SHELXL-97*, Universität Göttingen, **1997**.

Received April 25, 20001
[I01145]